Session VI

The Distant Universe

https://doi.org/10.1017/S0074180900196743 Published online by Cambridge University Press

Maps of the Cosmos
ASP Conference Series, Vol. 216, 2005
M. Colless, L. Staveley-Smith, R. Stathakis

High-Redshift Galaxies

Amy Barger

Department of Astronomy, University of Wisconsin-Madison, 475 N. Charter St., Madison, WI 53706

Department of Physics and Astronomy, University of Hawaii, 2505 Correa Road, Honolulu, HI 96822

Institute for Astronomy, University of Hawaii, 2680 Woodlawn Drive, Honolulu, HI 96822

Abstract. Mapping the history of star formation requires combining observations at many wavelengths. The most dramatic episodes of star formation occurred in high-redshift ($z > 1$) galaxies obscured by dust. These galaxies can be seen at submillimeter wavelengths. While these episodes clearly constitute much of the star formation in the universe, we still do not know the redshift distribution. Although progess has been made in determining the nature of the brightest members of the submillimeter population, these galaxies comprise only a tiny fraction of the submillimeter extragalactic background light. Optical star formation, by contrast, is well mapped but hard to interpret because of the problems of extinction. At recent times there is still substantial star formation, but it primarily takes place in small galaxies. This cosmic downsizing is paralleled by similar evolution in the properties of AGNs.

1. Introduction

A major goal of observational cosmology is to understand the star formation and accretion histories of the universe from the earliest times that cosmic structures formed until the present. To do so we need to obtain a complete census of all the energy-producing galaxies and supermassive black holes in the universe. A serious impediment has been that many luminous galaxies are hidden by dust from optical view. Fortunately, we are now able to find these highly obscured sources at X-ray, submillimeter, and radio wavelengths. Once we have accounted for the extragalactic background light (EBL), which is the accumulation of emission from all extragalactic sources along the line-of-sight, our census will be complete.

Figure 1 shows the bolometric EBL versus wavelength. Most of the energy produced in the universe emerges at far-infrared (FIR) and optical wavelengths. Only a small fraction of the total energy emerges in X-rays. However, since nearly all of the XRB arises from accretion onto supermassive black holes, X-ray surveys provide our best window on black hole evolution. In contrast, the optical background is produced primarily by star formation, and the FIR background by dust obscured star-forming galaxies and a smaller contribution of dust and gas obscured supermassive black holes.

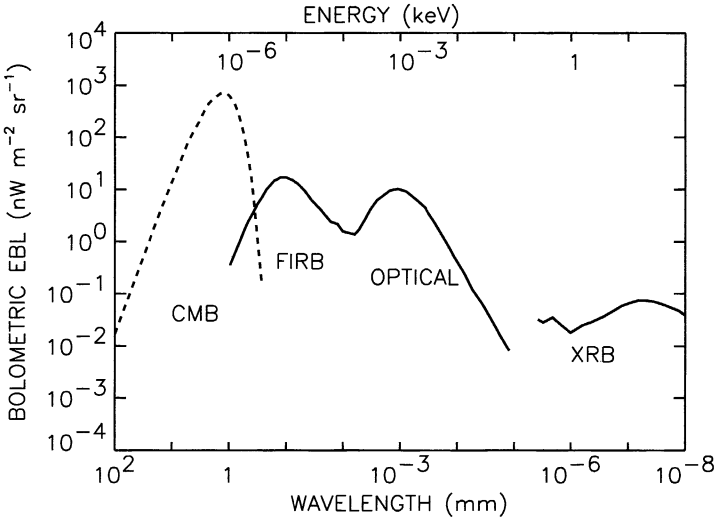

Figure 1. Schematic of the bolometric EBL versus wavelength. Dashed curve is the cosmic microwave background radiation (CMB). The far-infrared background (FIRB) has approximately the same integrated energy density as the optical EBL. The X-ray background (XRB) peaks at about 30 keV. An important observational goal is to resolve the backgrounds into their discrete components to obtain a census of star forming galaxies and supermassive black holes in the universe. Figure courtesy of Barger (2002).

2. Resolution of the Backgrounds

2.1. Submillimeter Background

The measurement of the EBL at FIR and submillimeter wavelengths using data from the *FIRAS* and *DIRBE* experiments on the *COBE* satellite (e.g., Puget et al. 1996; Fixsen et al. 1998) revealed a surprising result: the total emission from star formation and active galactic nuclei (AGN) activity that is absorbed by gas and dust and reradiated into the FIR/submillimeter is comparable to the total emission seen in the optical (Figure 1).

Reradiation of stellar light by dust in the FIR produces a thermal emission peak at $\lambda \sim 60 - 100$ μm that is redshifted into the submillimeter for galaxies at $z > 1$. Submillimeter observations are unique in that the strong negative K-corrections at 850 μm nearly compensate for cosmological dimming beyond $z \sim 1$, thereby making dusty galaxies almost as easy to detect at $z \sim 10$ as at $z \sim 1$ (Blain & Longair 1993).

The revolutionary Submillimeter Common User Bolometer Array (SCUBA; Holland et al. 1999) camera on the 15 m James Clerk Maxwell Telescope (JCMT) on Mauna Kea resolves the submillimeter EBL into its individual components through a combination of unparalleled sensitivity and large field-of-view. Deep submillimeter surveys with SCUBA have revealed a population of obscured galaxies with properties similar to those expected for distant counterparts to

https://doi.org/10.1017/S0074180900196743 Published online by Cambridge University Press

the most luminous, merging systems observed locally, the ultraluminous infrared galaxies (ULIGs, e.g., Arp 220; Sanders & Mirabel 1996).

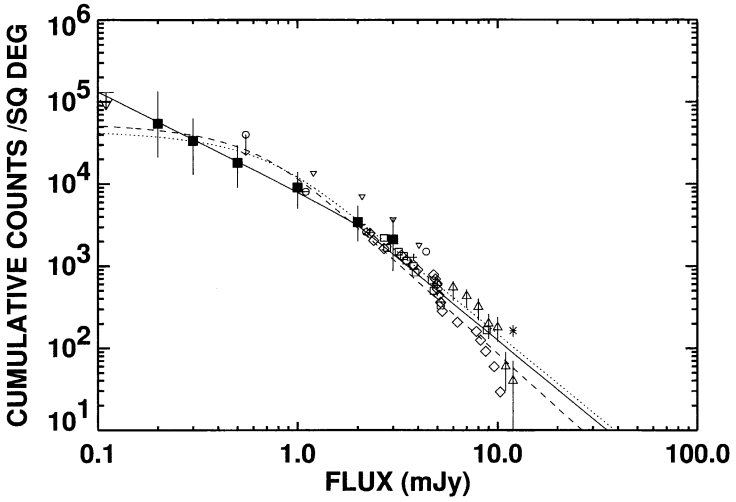

Figure 2. Cumulative number counts per square degree vs. 850 μm flux. From cluster lensing analyses: *solid squares*—Cowie et al. (2002a) between 0.2 and 3 mJy with 90% confidence limits; *open circles*—Blain et al. (1999) displaced to slightly larger fluxes for clarity; *downward-pointing triangles*—Chapman et al. (2002). From blank field analyses: *open diamonds*—Barger et al. (1999a); *crosses*—Hughes et al. (1998); *open squares*—Eales et al. (2000); *open triangles*—Scott et al. (2002) with 1σ uncertainties; *asterisk*—Borys et al. (2002). Dotted and dashed lines show, respectively, the parametric fits from Barger et al. (1999a) and from Cowie et al. (2002a), both of which integrate to match the EBL. A broken power law representation (*solid lines*) with slope -2 above 3 mJy and -1.2 below 3 mJy is divergent at faint fluxes and must turn over further at some point. Figure courtesy of Cowie et al. (2002a).

Figure 2 shows cumulative SCUBA galaxy counts per square degree versus 850 μm flux. Blank-field surveys with SCUBA have established the counts from 2 mJy to 10 mJy, which account for 20 to 30% of the 850 μm EBL (e.g., Barger et al. 1998; Hughes et al. 1998; Barger, Cowie, & Sanders 1999a; Lilly et al. 1999; Eales et al. 1999, 2000; Webb et al. 2003b, 2003c), depending on the EBL measurement used. Since the resolution of SCUBA is rather coarse (about 15″), blank-field surveys become confusion limited at fluxes below 2 mJy. To search for fainter submillimeter sources with SCUBA, one must therefore observe fields that contain massive clusters to take advantage of the gravitational magnification of background sources by these natural lenses. An additional advantage of observing lensed fields is that the confusion noise is reduced due to the expansion of the source plane. Smail, Ivison, & Blain (1997), and subsequently Chapman et al. (2002), were the first to try this approach with SCUBA using modest exposure times.

https://doi.org/10.1017/S0074180900196743 Published online by Cambridge University Press

Cowie, Barger, & Kneib (2002a) were able to probe to very faint submillimeter fluxes by obtaining ultradeep SCUBA observations of cluster fields—more than 2 to 5 times longer than any other published cluster field observations. From these data, Cowie et al. (2002a) directly measured the source contribution in the 0.3 mJy to 2 mJy flux range to be $2.0^{+3.2}_{-0.8} \times 10^4$ mJy deg^{-2}, where the upper and lower bounds are the 90% confidence range. This corresponds to 45 to 65% of the 850 μm, depending on the EBL measurement used. Given that 20 to 30% of the EBL is resolved at flux densities between 2 mJy and 10 mJy, most of the 850 μm EBL must arise in sources above 0.3 mJy. The surface density at these faint fluxes enters the realm of significant overlap with other galaxy populations (see § 3).

2.2. X-ray Background

The X-ray background (XRB; Giacconi et al. 1962) was the first cosmic background radiation discovered (even before the cosmic microwave background). *ROSAT* resolved 70 to 80% of the soft ($0.5 - 2$ keV) XRB into discrete sources (Hasinger et al. 1998), most of which were optically identified as unobscured AGNs (Schmidt et al. 1998). In obscured sources the optical light through soft X-rays are absorbed; thus, hard ($2 - 8$ keV) X-ray observations are needed, since these photons are able to penetrate the obscuring gas and dust. Although most of the energy density in the XRB resides at energies above 2 keV, only recently have technological developments in X-ray detectors made it possible to resolve greater than 80 to 90% of the $2 - 8$ keV XRB into discrete sources using the *Chandra* and *XMM-Newton* X-ray satellites (e.g., Mushotzky et al. 2000; Campana et al. 2001; Cowie et al. 2002b; Rosati et al. 2002; Alexander et al. 2003; Hasinger et al. 2001).

Cowie et al. (2002b) noticed large variance in the *Chandra* source counts on scales of $\sim$ 100 arcmin^2. The origin of the variance is not known, but it is likely due to cosmic variance originating in large scale structure. Redshift measurements of the sources in two ultradeep *Chandra* images have also found large scale structure in the form of velocity sheets (Barger et al. 2003; Gilli et al. 2003). Because the angular size of the large scale structure is on the order of a single *Chandra* pointing, Yang et al. (2003) used a wide-field, moderately deep *Chandra* survey of the Lockman Hole-North West (LH-NW) region to measure the autocorrelation function of the X-ray sources. These authors found that the full range of cosmic variance seen in the earlier, individual *Chandra* pointings was represented in the number counts of the nine LH-NW pointings. They found the clustering in both the hard and soft X-ray bands to be significant, though, interestingly, the X-ray sources detected only in the hard band appear to be substantially more clustered.

3. Submillimeter Source Properties

3.1. Identification of Optical/Near-infrared Counterparts

It is often difficult to identify the optical/near-infrared (NIR) counterparts to the submillimeter sources due to the coarse resolution of SCUBA and the intrinsic faintness of the sources. Barger et al. (1999b) presented a spectroscopic survey

of all possible optical counterparts to the submillimeter sources in the flux-limited lensed cluster survey of Smail et al. (1998). They used moderately deep ground-based and *HST* images ($I \sim 23.5$ and $I \sim 26$, respectively) to identify all candidate optical counterparts within the SCUBA error circles and then followed-up these sources spectroscopically with LRIS (Oke et al. 1995) on Keck. Their ability to conclude whether a particular galaxy was likely to be the true optical counterpart depended strongly on whether the optical spectrum of the galaxy showed any remarkable features, such as particularly strong [OII] λ3727 or Hα emission lines that would indicate a starburst galaxy, or high excitation or broad emission lines that would mark the presence of an AGN. The relative paucity of AGNs in the general field population ($< 1\%$, as identified from optical spectra as opposed to X-ray emission) suggests that if an AGN is identified, then the submillimeter emission is most likely associated.

Barger et al. (1999b) reliably spectroscopically identified one-quarter of the submillimeter sources. However, for the remaining sources, either there were no visible optical counterparts in the images used (the regions within the error circles were optically 'blank'), or the associations of the submillimeter sources with the optical sources were not secure.

Even though the counterparts to the submillimeter sources are often optically faint, in many cases they can still be detected in the NIR due to their dusty, highly reddened nature. For example, deep NIR imaging of the Smail et al. (2002) and Cowie et al. (2002a) $> 4\sigma$ lensed submillimeter samples have revealed a number of such counterparts, including a source recently found to lie at $z = 2.51$ (Frayer et al. 2003; it shows weak AGN signatures) from a NIR spectrum.

3.2. Relation to Extremely Red Objects

The identification of counterparts with such unusually red colors (called extremely red objects, or EROs, if $I - K > 4$, and very red objects, or VROs, if $3.5 < I - K < 4$) to the submillimeter sources led Wehner, Barger, & Kneib (2002) to statistically measure the average submillimeter flux of the ERO and VRO populations in order to determine their contributions to the submillimeter EBL. They used the ultradeep submillimeter and NIR data of the three massive lensed cluster fields of Cowie et al. (2002a) and found that, on average, the ERO (1.58 ± 0.13 mJy) and VRO (1.32 ± 0.19 mJy) populations mark strong submillimeter emitters. In fact, the two populations together contribute $2.59 \pm 0.19 \times 10^4$ mJy deg^{-2}, which corresponds to about 60 to 80% of the 850 μm EBL, depending on the EBL measurement used. (The issue of clustering among EROs is clearly an important effect, which must be taken into account to obtain a better estimate; see also Takata et al. 2003.) The error-weighted mean submillimeter fluxes of the ERO and VRO populations are marked in Figure 3, which shows the flux contributions to the 850 μm EBL using the parametric fit of Cowie et al. (2002a).

In addition, Wehner et al. (2002) found that the mean 850 μm flux per source decreases with source plane K' magnitude. Since submillimeter flux depends only weakly on redshift, higher redshift sources should appear fainter in K' but not in 850 μm flux. The above result is therefore contrary to expectations. It suggests that sources that are fainter in K' are intrinsically fainter in

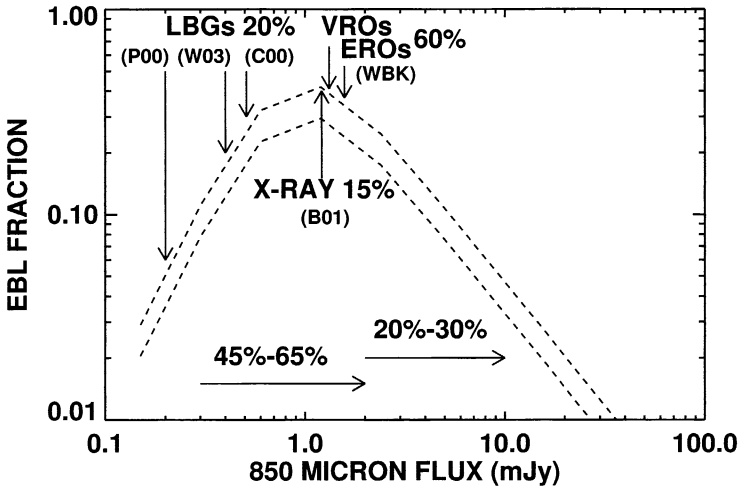

Figure 3. Contributions to the 850 μm EBL vs. 850 μm flux. Dashed curves show the parametric fit of Cowie et al. (2002a). Statistical measurements of the submillimeter properties of LBGs (Peacock et al. 2000; Webb et al. 2003a; Chapman et al. 2000), X-ray sources (Barger et al. 2001a), and EROs and VROs (Wehner et al. 2002) are marked with vertical arrows, and their approximate percent contributions to the EBL are noted. The fraction of the 850 μm EBL resolved in specific flux intervals are marked with horizontal arrows and labels. Figure courtesy of Barger (in preparation).

850 μm luminosity. This dependence of the submillimeter flux on the K' magnitude also means that brighter submillimeter surveys are more likely to identify ERO counterparts to their submillimeter galaxies. Wehner et al. (2002) found that the median magnitude of the sources giving rise to the EBL is $K' = 20$ to $K' = 20.3$, depending on the cluster sample used.

3.3. Relation to Lyman Break Galaxies

High-redshift star-forming galaxies are routinely identified photometrically from the redshifted continuum spectral discontinuity at 912 Å and the flat continuum longward of the redshifted Lyα line (Cowie et al. 1988). This so-called "Lyman-break" technique has enabled the efficient selection of galaxies over the redshift range $2 < z < 4$ (e.g., Steidel et al. 1996), and hence the mapping of the star formation rate density at high redshifts (e.g., Madau et al. 1996; see § 6). Discerning the relationship between the Lyman-break galaxies (LBGs) and the submillimeter galaxies is a necessary step for understanding the evolutionary history of the two populations.

The successful optical spectroscopic identification of a few of the submillimeter galaxies due to their sufficiently bright UV luminosities led Adelberger & Steidel (2000) to propose that galaxies similar to those detected in the Lyman-break surveys produce the bulk of the measured 850 μm background. One

https://doi.org/10.1017/S0074180900196743 Published online by Cambridge University Press

approach to determining how much the LBG population contributes to the submillimeter background is to look for positive background fluctuations in deep 850 μm images to see if they are coincident with the locations of UV-selected high-redshift galaxies. Peacock et al. (2000) were the first to try this using the ultradeep 850 μm SCUBA map of the HDF-N obtained by Hughes et al. (1998). Their statistical detection of the submillimeter flux from galaxies with high UV luminosities, and hence high star formation rates, was about 0.2 mJy for an apparent UV star formation rate of 1 h^{-2} $M_\odot$ yr^{-1}. They found this level of submillimeter emission to be consistent with the idea that the UV emission from LBGs underestimates the total star formation rate by a mean factor of about six. Thus, they concluded that the LBG population must contribute at least 25% to the 850 μm EBL.

Other statistical studies of LBGs obtained similar levels of submillimeter emission. Chapman et al. (2000) measured an error-weighted mean 850 μm flux of 0.51 ± 0.39 mJy from their SCUBA photometry sample of eight LBGs. Webb et al. (2003a) measured the submillimeter fluxes of LBGs in their SCUBA jiggle maps of three fields and marginally ($\sim 2\sigma$) detected mean submillimeter fluxes of 0.414 ± 0.263 mJy and 0.382 ± 0.206 mJy from two of the samples but obtained no detection from the third sample. Webb et al. (2003a) placed an upper limit on the LBG contribution to the 850 μm background at around 20% by assuming that LBGs have a constant comoving number density between $z = 1$ and 5. The error-weighted mean 850 μm fluxes of the LBGs measured by the three groups are shown in Figure 3. Clearly this population cannot be the dominant contributor to the submillimeter background.

4. Radio-Submillimeter Association

High-resolution centimeter continuum maps with subarcsecond positional accuracy and resolution provide new opportunities for locating submillimeter sources and determining their physical properties. The unique advantage of centimeter observations is that galaxies and the intergalactic medium are transparent at these wavelengths, so observed flux densities are proportional to intrinsic luminosities. In galaxies without a powerful AGN, the radio luminosity is dominated by diffuse synchrotron emission and probes very recent star formation. Radio continuum emission and thermal dust emission are empirically observed to be tightly correlated as a result of both being linearly related to the massive star formation rate (Condon 1992).

Using the combination of SCUBA data and an ultradeep 1.4 GHz map obtained with the Very Large Array (VLA) of the HDF-N region (Richards 2000), Barger, Cowie, & Richards (2000) found that a radio pre-selection technique can identify bright (> 6 mJy) submillimeter sources without the need for long submillimeter exposures. These authors found that about 65% of bright submillimeter sources have 1.4 GHz counterparts to a radio flux limit of 40 μJy (5σ), a result which was later confirmed by Chapman et al. (2003b) and Ivison et al. (2002; for an 8 mJy sample).

Moreover, the precise radio astrometry enables counterparts to be readily identified. Chapman et al. (2003b) analyzed ultradeep radio and submillimeter jiggle map data of three fields and found that about 70% of the radio-

submillimeter sources have $I > 23.5$. These authors also used a statistical approach and found that both the optically bright and the optically faint microjansky radio sources are very significantly detected in the submillimeter, with error-weighted mean 850 μm fluxes of 1.05 ± 0.13 mJy and 2.76 ± 0.15 mJy, respectively.

Another advantage of radio data is that the ratio of the submillimeter flux to the radio flux can be used as a millimetric redshift estimator (Carilli & Yun 1999, 2000; Barger et al. 2000; Dunne, Clements, & Eales 2000; Rengarajan & Takeuchi 2001). When this technique is employed, most of the distant submillimeter sources are found to lie in the redshift range $z = 1 - 3$.

Since the radio images provide excellent positional accuracy, an interesting question to ask is how many of the submillimeter-detected radio sources can be spectroscopically identified. Chapman et al. (2003a) undertook spectroscopic observations of a sample of 34 radio-detected bright (> 5 mJy) submillimeter galaxies and were able to measure redshifts for ten. These lie in the redshift range $z = 0.8 - 3.7$. However, the optical faintness of many of the counterparts makes this a difficult task. We illustrate this in Figure 4, which shows redshift versus R magnitude for the radio sources in the HDF-N region. Large squares denote submillimeter sources that were significantly ($> 3\sigma$) detected in our jiggle-map observations of this region, most of which are very optically faint ($R > 24$).

Although redshifts can be obtained for some of the radio-detected bright submillimeter galaxies, it is important to keep in mind that the bright (> 5 mJy) submillimeter source population comprises only a tiny fraction of the submillimeter EBL (see Figure 3). Thus, any redshift distribution determined for this population is not necessarily the same redshift distribution as that of the dominant ~ 1 mJy source population.

The downside of using flux-limited radio surveys to study submillimeter galaxies is that a radio luminosity bias is introduced with redshift. This bias can be seen in Figure 5, which shows 1.4 GHz luminosity versus redshift for the microjansky radio samples in the HDF-N (Richards 2000) and SSA13 (Fomalont et al., in preparation) regions. The dotted curve shows the 40 μJy (5σ) radio flux limit of the HDF-N sample. (The 5σ radio flux limit of the SSA13 sample is 25 μJy, but there are only 7 sources in this sample between 25 and 40 μJy, and only one of these has a redshift identification.) Thus, at low redshifts ($z < 0.5$), Milky-Way type galaxies can be detected, at intermediate redshifts, luminous infrared galaxies (LIGs) can be detected, and at high redshifts ($z > 1.5$), only sources with luminosities above $10^{12}\ L_\odot$ (ULIGs; solid line shows the radio power that would locally correspond to this luminosity) can be detected in a radio flux-limited sample. The remaining 35% of the bright submillimeter population that were not detected in the radio, whose luminosities would be $> 4 \times 10^{12}\ L_\odot$ if their redshifts were $z > 1$, may therefore lie at redshifts $z > 3$.

It is also interesting to note from Figure 5 the rapid evolution in the upper bound of the radio power. This is the well-known effect called cosmic downsizing (Cowie et al. 1996), whereby galaxies at higher redshifts have very large star formation rates, while at lower redshifts the rates turn down rapidly. This can also be understood as extreme evolution in the ULIG number density: ULIGs are very rare at low redshifts, but the number density of ULIGs rises rapidly with redshift so that they are relatively common by $z = 1$ (see § 6).

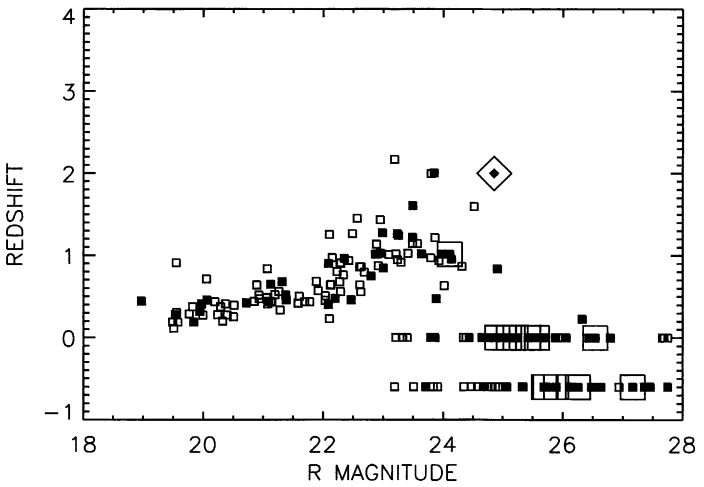

Figure 4. Redshift vs. R magnitude for the HDF-N radio sample. Sources without spectroscopic redshifts are plotted at or below $z = 0$. Solid squares have submillimeter observations, open squares do not. Large squares denote sources significantly ($> 3\sigma$) detected in the submillimeter, most of which are very optically faint. Spectroscopic observations by Barger et al. (2001a) of the X-ray sources in the 1 Ms *Chandra* Deep Field-North yielded a redshift for one submillimeter source at $z = 1.013$. Large open diamond denotes a source outside our submillimeter jiggle-map area detected by Chapman et al. (2003a) in SCUBA photometry mode.

5. AGN Contribution to the Submillimeter EBL

Any attempt at tracing the dust-obscured star formation history of the universe requires knowledge of the extent of the contribution that AGN make to powering the submillimeter sources. The existing spectroscopic identifications of bright submillimeter sources make one thing clear: there is a strong bias towards AGNs. The reasons for this bias are that the presence of an AGN makes the counterpart more optically luminous, and an AGN spectrum is easier to spectroscopically identify due to its strong emission-line features.

X-ray observations provide an unbiased avenue for determining the AGN contribution to the submillimeter EBL. Early searches for submillimeter counterparts to *Chandra* X-ray sources yielded mixed results due to the small areas with both submillimeter and X-ray data (Fabian et al. 2000; Bautz et al. 2000; Hornschemeier et al. 2000; Barger et al. 2001b) and the shallow depths of the X-ray images. The deepest X-ray image to date, the 2 Ms CDF-N exposure, reveals that more than 50% of the bright submillimeter-detected radio sources are also detected in X-rays (Wang et al., in preparation).

To determine the actual AGN contribution to the submillimeter EBL, one can again invert the procedure and do a statistical analysis. Barger et al. (2001a)

https://doi.org/10.1017/S0074180900196743 Published online by Cambridge University Press

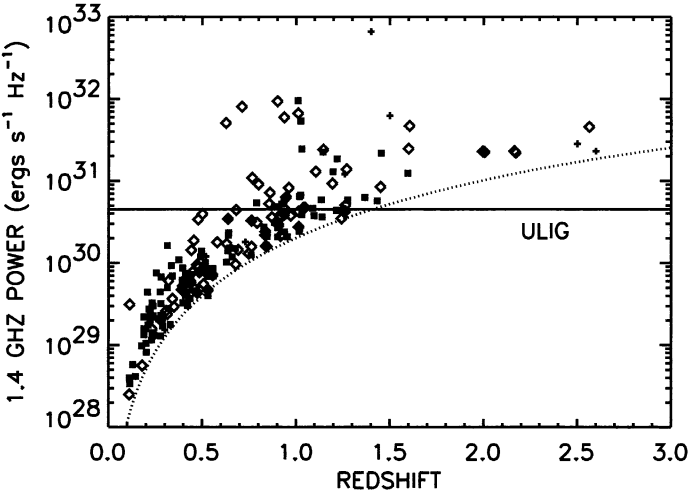

Figure 5. Rest-frame 1.4 GHz power versus redshift for the combined HDF-N and SSA13 radio samples (*open diamonds*—AGNs; *solid squares*—star-forming galaxies; *plus signs*—photometric redshifts). Dotted line shows the power corresponding to the 40 μJy flux limit of the HDF-N sample. Solid line shows the equivalent radio power of an $L_{FIR} = 10^{12}\ L_{\odot}$ source. Figure courtesy of Cowie et al. (2004).

analyzed submillimeter observations of 135 of the 370 X-ray sources detected in the 1 Ms exposure of the CDF-N and found a significant excess 850 μm flux (1.21 ± 0.27 mJy) associated with the ensemble of X-ray sources. This measurement is shown in Figure 3. Since most of the flux density from the *Chandra* sources arises from AGN activity, Barger et al. (2001a) estimated the AGN contribution to the 850 μm EBL to be between 12 and 16%, depending on the EBL measurement used. The submillimeter excess was found to be strongest in the optically faint X-ray sources that are also seen at 1.4 GHz, which is consistent with these X-ray sources being obscured and at high redshift ($z > 1$).

Similar results were obtained in subsequent analyses by Waskett et al. (2003) using two 50 ks *XMM-Newton* exposures (the noise-weighted mean 850 μm fluxes were 0.48 ± 0.27 mJy and 0.35 ± 0.28 mJy) and Almaini et al. (2003) using an 150 ks *Chandra* exposure (the noise-weighted mean flux was 0.89 ± 0.3 mJy). The small AGN contribution to the submillimeter EBL is easily understood on energetic grounds and was predicted by Gunn & Shanks (1998), Fabian & Iwasawa (1999), and Almaini, Lawrence, & Boyle (1999). Thus, most of the submillimeter EBL is probably due to star formation, though there may be some Compton-thick AGN contributions that are missed in the $2 - 8$ keV X-ray surveys.

https://doi.org/10.1017/S0074180900196743 Published online by Cambridge University Press

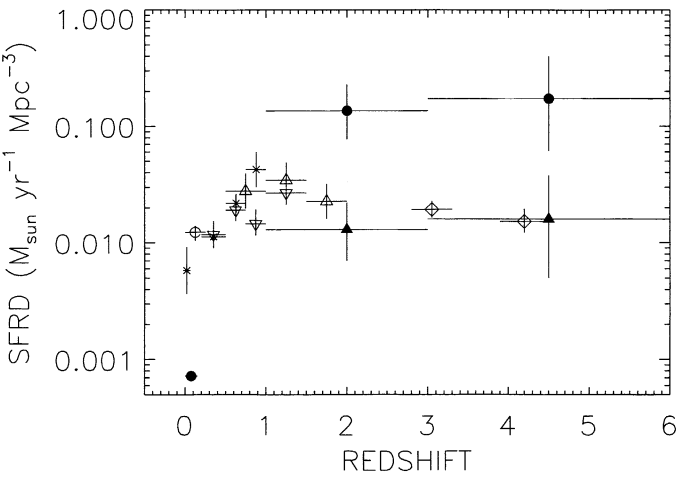

Figure 6. Star formation rate density vs. redshift. Submillimeter results for fluxes > 6 mJy are shown as filled triangles, and the results corrected for completeness are shown as filled circles. Uncertainties are Poissonian based on the number of sources. Local point (*filled circle*) is based on ULIG data from Kim & Sanders (1998) and near-ULIG data from Sanders et al. (2003). All optical and ultraviolet points are uncorrected for extinction: *open circle*—Treyer et al. (1998); *asterisks*—Lilly et al. (1996); *open upside-down triangles*—Cowie, Songaila, & Barger (1999); *open triangles*—Connolly et al. (1997); *open diamonds*—Steidel et al. (1999). Figure courtesy of Barger et al. (2000).

6. Dust-Obscured Star Formation History

Observations of high-redshift sources are often interpreted using the comoving volume-averaged history of star formation diagram introduced by Madau et al. (1996). Measurements are typically based on the rest-frame UV luminosity function, whose origin is assumed to be young stellar populations. However, the UV emission from a galaxy is heavily affected by the presence of even small amounts of dust, and extinction corrections are highly uncertain. FIR and radio luminosities provide a direct measure of the current star formation rate (SFR) in a galaxy and hence can be used to obtain the dust-obscured star formation history.

Since most of the submillimeter EBL is probably produced by star formation instead of AGN activity (see § 5), we can use the SCUBA observations to infer the dusty star formation history. The 850 μm flux maps directly to luminosity for $z > 1$ (the brightening of the K-correction balances the luminosity distance term; see § 2.1), so we only need to know the redshifts very roughly (i.e., the volume that the sources occupy) to map the star formation history. We can use either the spectroscopic redshifts or crude millimetric redshift estimates, which place most of the submillimeter sources in the range $z = 1 - 3$, or just estimate

https://doi.org/10.1017/S0074180900196743 Published online by Cambridge University Press

the approximate redshift range from the spectral shape of the submillimeter EBL (Gispert, Lagache, & Puget 2000).

Figure 6 shows the star formation rate density (SFRD) versus redshift. The solid triangles show the submillimeter contribution to the SFRD inferred from the > 6 mJy observations of Barger et al. (2000). This is seen to be comparable to the UV/optical contribution to the SFRD (*open symbols*) at these redshifts. The completeness corrected submillimeter SFRD, which assumes that the flux to FIR luminosity conversion based on Arp 220 applies in the low submillimeter flux region, is shown by the filled circles. The justification for this assumption is that even the dominant ~ 1 mJy population have roughly ULIG luminosities. The completeness correction over all submillimeter fluxes is just the measured 850 μm EBL divided by the 850 μm light above 6 mJy. The correction factors are 11 and 15, respectively, for the Puget et al. (1996) and Fixsen et al. (1998) EBL measurements.

From Figure 6 we see that the >6 mJy sources only contribute a small fraction of the SFRD and that most of the SFRD is due to sources with fluxes around 1 mJy. As long as these fainter sources are star formation dominated, then the SFRD estimate should be good. Although neither millimetric redshift estimates nor optical spectroscopy are easy to do for these fainter sources, as mentioned above, the precise redshifts are not critical for determining the star formation history.

The completeness-corrected SFRD shows a very rapid evolution in the SFRD of ULIGs from $z \sim 0$ to $z \sim 1-3$, but it would be nice to be able to measure this evolution directly at $z < 1.5$. With present detection capabilities, the radio provides greater sensitivity to SFRs at low redshifts than the submillimeter. This can be seen from Figure 5: at redshifts $z > 1.5$ the submillimeter currently provides the only access to distant ULIGs, while at redshifts $z < 1.5$, the radio provides the best means for accurately measuring the SFRs of galaxies.

In Figure 7 we show the number density of star-forming galaxies with ULIG radio powers in three redshift intervals (*solid squares*). The open square denotes the local value from various determinations of the local radio luminosity function (Condon 1989; Sadler et al. 2002; Machalski & Godlowski 2001). The evolution is reasonably well-described by a $(1+z)^7$ evolution (*dashed line*). This evolution is similar to that inferred from a comparison of the local number density of ULIGs and near-ULIG to the number density of $z = 1-3$ radio-detected ULIGs inferred from > 6 mJy submillimeter observations by Barger et al. (2000; *solid circles*), as would be expected if both the radio galaxies classified as star formers and the submillimeter sources are indeed dominated by star formation.

7. Summary

Deep submillimeter surveys offer an unobscured view of dust-enshrouded star formation or AGN activity at high redshifts and are crucial for understanding the cosmic star formation history. Progress has been made in resolving and understanding the nature of the bright submillimeter source population, and even a crude redshift distribution has been obtained via direct spectroscopic measurements (many exhibit AGN characteristics) or millimetric redshift estimates

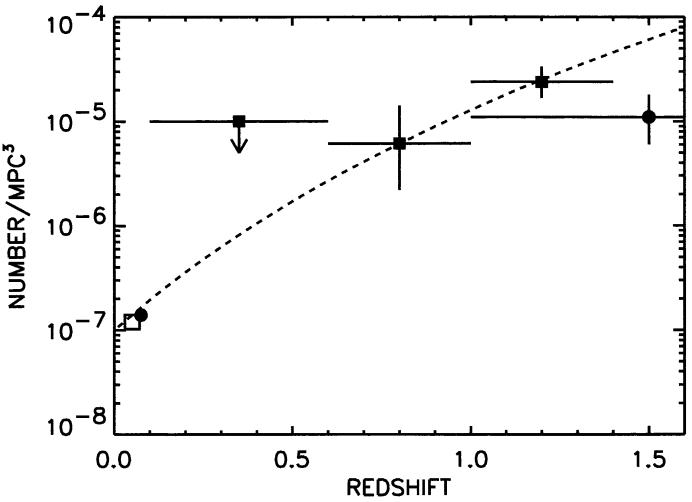

Figure 7. Number density of star-forming galaxies with ULIG radio powers in the redshift intervals $z = 0.1 - 0.6$, $z = 0.6 - 1.0$, and $z = 1.0 - 1.4$ (*solid squares*). Open square denotes the local value from the various determinations of the local radio luminosity function (see text for references). Solid circles denote the local density of ULIGs and near-ULIGs from Kim & Sanders (1998) and Sanders et al. (2003), as calculated by Barger et al. (2000), and the > 6 mJy radio-detected submillimeter ULIG space density in the redshift interval $z = 1 - 3$ from Barger et al. (2000). Dashed line shows a $(1 + z)^7$ evolution. Figure courtesy of Cowie et al. (2004).

obtained from the submillimeter to radio flux ratios. A flux-limited radio survey unfortunately introduces a radio luminosity bias with redshift, so one is only probing the most luminous systems at each redshift. Moreover, the bright submillimeter sources contribute only a tiny fraction to the submillimeter EBL and require more than a factor of 10 correction to obtain the dusty star formation history.

It is the $\sim$1 mJy at 850 μm sources that dominate the EBL, and their redshift distribution and source characteristics could be different than those of the bright submillimeter sources. Statistical measurements have given us some insight into the nature of these sources. For example, LBGs can overlap with the submillimeter sources only at the faintest submillimeter fluxes and hence cannot be the dominant contributors to the submillimeter EBL; their contribution is measured to be about 20%. AGNs and EROs/VROs overlap at fluxes > 1 mJy, but AGNs still only contribute about 15% to the EBL, whereas EROs/VROs contribute at a much higher level of about 60%.

Currently the ~ 1 mJy sources can only be detected with SCUBA through the gravitational lensing effects of intervening massive clusters of galaxies. The Submillimeter Array (SMA) on Mauna Kea will provide several advances in the near future. First, it will enable accurate positions to be obtained for the

https://doi.org/10.1017/S0074180900196743 Published online by Cambridge University Press

bright SCUBA sources; this will prove especially useful for those sources without radio counterparts. Second, in a few years time, it will have the sensitivity to perform blank-field observations and should directly detect the $\sim$ 1 mJy source population. Ultimately, observations with ALMA will routinely detect the dominant $\sim$ 1 mJy population and hence enable a complete reconstruction of the star formation history of the universe.

Acknowledgments. I thank Lister Staveley-Smith and John Peacock for inviting me to participate in this stimulating symposium. I gratefully acknowledge support from CXC grant GO2-3191A, NSF grant AST 00-84847, the University of Wisconsin Research Committee, and the Alfred P. Sloan Foundation.

References

Adelberger, K. L., & Steidel, C. C. 2000, ApJ, 544, 218
Alexander, D. M., et al. 2003, AJ, 126, 539
Almaini, O., et al. 2003, MNRAS, 338, 303
Almaini, O., Lawrence, A., & Boyle, B. J. 1999, MNRAS, 305, L59
Barger, A. J. 2002, Contemporary Physics, 43, 339
Barger, A. J., Cowie, L. L., Mushotzky, R. F., & Richards, E. A. 2001b, AJ, 121, 662
Barger, A. J., Cowie, L. L., & Richards, E. A. 2000, AJ, 119, 2092
Barger, A. J., Cowie, L. L., & Sanders, D. B. 1999a, ApJ, 518, L5
Barger, A. J., et al. 1998, Nature, 394, 248
Barger, A. J., et al. 1999b, AJ, 117, 2656
Barger, A. J., et al. 2001a, ApJ, 560, L23
Barger, A. J., et al. 2003, AJ, 126, 632
Bautz, M. W., et al. 2000, ApJ, 543, L119
Blain A.W., Kneib J.-P., Ivison R.J., & Smail I. 1999, ApJ, 512, L87
Blain, A. W., & Longair, M. S. 1993, MNRAS, 264, 509
Borys, C., Chapman, S. C., Halpern, M., & Scott, D. 2002, MNRAS, 330, L63
Campana, S., Moretti, A., Lazzati, D., & Tagliaferri, G. 2001, ApJ, 560, L19
Carilli, C. L., & Yun, M. S. 1999, ApJ, 513, L13
Carilli, C. L., & Yun, M. S. 2000, ApJ, 530, 618
Chapman, S. C., Blain, A. W., Ivison, R. J., & Smail, I. R. 2003a, Nature, 422, 695
Chapman, S. C., et al. 2000, MNRAS, 319, 318
Chapman, S. C., et al. 2003b, ApJ, 585, 57
Chapman, S. C., Scott, D., Borys, C., & Fahlman, G. G. 2002, MNRAS, 330, 92
Condon, J. J. 1989, ApJ, 338, 13
Condon, J. J. 1992, ARA&A, 30, 575
Connolly, A.J., Szalay, A.S., Dickinson, M., SubbaRao, M.U., & Brunner, R.J. 1997, ApJ, 486, L11
Cowie, L. L., Barger, A. J., Fomalont, E. B., & Capak, P. 2004, ApJ, 603, L69
Cowie, L. L., Barger, A. J., & Kneib, J.-P. 2002a, AJ, 123, 2197
Cowie, L. L., et al. 2002b, ApJ, 566, L5
Cowie, L. L., Lilly, S. J., Gardner, J., & McLean, I. S. 1988, ApJ, 332, L29
Cowie, L.L., Songaila, A., & Barger, A.J. 1999, AJ, 118, 603
Cowie, L. L., Songaila, A., Hu, E. M., & Cohen, J. G. 1996, AJ, 112, 839

Dunne, L., Clements, D. L., & Eales, S. A. 2000, MNRAS, 319, 813
Eales, S., et al. 1999, ApJ, 515, 518
Eales, S., et al. 2000, AJ, 120, 2244
Fabian, A. C., et al. 2000, MNRAS, 315, L8
Fabian, A. C., & Iwasawa, K. 1999, MNRAS, 303, L34
Fixsen, D. J., Dwek, E., Mather, J. C., Bennett, C. L., & Shafer, R. A. 1998, ApJ, 508, 123
Frayer, D. T., et al. 2003, AJ, 126, 73
Giacconi, R., Gursky, H., Paolini, F. & Rossi, B. 1962, Phys.Rev.Lett, 9, 439
Gilli, R., et al. 2003, ApJ, 592, 721
Gispert, R., Lagache, G., & Puget, J. L. 2000, A&A, 360, 1
Gunn, K. F., & Shanks, T. 1998, Astron. Nach., 319, 66
Hasinger, G., et al. 1998, A&A, 329, 482
Hasinger, G., et al. 2001, A&A, 365, L45
Holland, W. S., et al. 1999, MNRAS, 303, 659
Hornschemeier, A. E., et al. 2000, ApJ, 541, 49
Hughes, D. H., et al. 1998, Nature, 394, 241
Ivison, R. J., et al. 2002, MNRAS, 337, 1
Kim, D. -C., Sanders, D. B. 1998, ApJS, 119, 41
Lilly, S. J., et al. 1999, ApJ, 518, 641
Lilly, S. J., Le Fèvre, O., Hammer, F., & Crampton, D. 1996, ApJ, 460, L1
Machalski, J., & Godlowski, W. 2001, A&A, 370, 923
Madau, P., et al. 1996, MNRAS, 283, 1388
Mushotzky, R. F., Cowie, L. L., Barger, A. J., & Arnaud, K. A. 2000, Nature, 404, 459
Oke, J. B., et al. 1995, PASP, 107, 375
Peacock, J. A., et al. 2000, MNRAS, 318, 535
Puget, J. -L., et al. 1996, A&A, 308, L5
Rengarajan, T. N., & Takeuchi, T. T. 2001, PASJ, 53, 433
Richards, E. A. 2000, ApJ, 533, 611
Rosati, P., et al. 2002, ApJ, 566, 667
Sadler, E. M., et al. 2002, MNRAS, 329, 227
Sanders, D. B., Mazzarella, J. M., Kim, D.-C., Surace, J. A., & Soifer, B. T. 2003, AJ, 126, 1607
Sanders, D. B., & Mirabel, I. F. 1996, ARA&A, 34, 749
Schmidt, M., et al. 1998, A&A, 329, 495
Scott, S. E., et al. 2002, MNRAS, 331, 817
Smail, I., Ivison, R. J., & Blain, A. W. 1997, ApJ, 490, L5
Smail, I., Ivison, R. J., Blain, A. W., & Kneib, J. -P. 1998, ApJ, 507, L21
Smail, I., Ivison, R. J., Blain, A. W., & Kneib, J. -P. 2002, MNRAS, 331, 495
Steidel, C. C., Adelberger, L., Giavalisco, M., Dickinson, M., & Pettini, M. 1999, ApJ, 519, 1
Steidel, C. C., Giavalisco, M., Pettini, M., Dickinson, M., & Adelberger, K. L. 1996, ApJ, 462, L17
Takata, T., et al. 2003, PASJ, 55, 789
Treyer, M. A., Ellis, R. S., Milliard, B., Donas, J., & Bridges, T. J. 1998, MNRAS, 300, 303
Waskett, T. J., et al. 2003, MNRAS, 341, 1217

Webb, T. M., et al. 2003a, ApJ, 582, 6
Webb, T. M., et al. 2003b, ApJ, 587, 41
Webb, T. M., et al. 2003c, ApJ, 597, 680
Wehner, E. H., Barger, A. J., & Kneib, J. -P. 2002, ApJ, 577, L83
Yang, Y., et al. 2003, ApJ, 585, L85